J Mol Model (2007) 13:731–737
DOI 10.1007/s00894-007-0189-4

ORIGINAL PAPER

Modeling the adsorption of aromatic compounds on the TiO_2/SiO_2 catalyst

Bartłomiej Szyja · Krzysztof Brodzik

Received: 31 October 2006 / Accepted: 15 February 2007 / Published online: 6 March 2007

Abstract The Grand Canonical Monte Carlo method was used to analyse the phenomenon of adsorption of aromatic compounds (i.e. phenol, toluene, benzoic acid and salicylic acid) on the surface of the titania-silica (TiO_2/SiO_2) catalyst. We found that different types of interactions play important roles in the adsorption of molecules having polar and non-polar groups. Moreover, we found that the interactions between sorbate molecules are strong, and are the cause of multilayer adsorption occurring in the investigated temperature and pressure range.

Keywords Sorption · Grand Canonical Monte Carlo · Titania-silica

Introduction

Extensive studies on the applications of titanium dioxide in the field of photocatalysis began in 1972 when Fujishima and Honda achieved photo-induced water cleavage on a TiO_2 photoanode [1, 2]. Since then, TiO_2 is one of most frequently studied photocatalysts, and is often used as a reference material in photocatalysis due to its favourable band gap energy and high chemical stability. Studies of titanium dioxide as a photocatalyst include, among others, photodecomposition of water to produce hydrogen, photocatalytic decomposition of organic compounds as well as photocatalytic sterilization or cancer treatment [3–6]. Applications in the field of photocatalytic degradation of organic compounds—an example of an advanced oxidation process (AOP)—take advantage of the possibility of total mineralisation of pollutants. In the case of decomposition of aromatic compounds, some intermediate species can be generated but when an aromatic ring is broken, photodegradation leads to very rapid mineralisation of aliphatic derivatives [7].

Photocatalytic studies point to two forms of TiO_2 crystals that can be used as photocatalysts: anatase and rutile. Pure anatase is in general more photocatalytically effective than pure rutile; however, some mixtures of anatase and rutile show even higher activities than pure anatase alone [8, 9]. The photocatalyst can be made more effective not only by tailoring its crystalline form, but also by introducing other oxides. Xu et al. studied the photoactivity of titania-silica (TiO_2/SiO_2) aerogels in comparison with pure titania aerogels [10], and concluded that the textural properties of the photocatalyst, such as porosity or specific surface area, were highly enhanced by the presence of a well developed silica matrix. Use of silica should also ensure better accessibility of titania particles, hence their better utilisation.

Adsorption of pollutants was found to be one of the major factors determining photocatalytic activity, therefore it is very important to know what factors influence this process. Bhatkhande et al. [7] reviewed the influence of preadsorbed organic compounds on the extent of their total degradation. In the case of photodegradation of volatile organic compounds (VOC), adsorption occurs from the gas phase. It is obvious that photodegradation of easily adsorbable species is faster than that of other, less adsorbable compounds.

Presented at: Modeling and Design of Molecular Materials, 10–15 September 2006, Wrocław, Poland.

B. Szyja (✉) · K. Brodzik
Faculty of Chemistry,
Wrocław University of Technology,
ul. Gdańska 7/9,
50-344 Wrocław, Poland
e-mail: sbart@pwr.wroc.pl

Titania-silica aerogels are highly porous materials obtained by using a sol-gel process followed by supercritical drying. Their method of production allows the properties and composition of these materials to be tailored over a very wide range. In such materials, it is important that titania is connected with silica via Ti–O–Si bonding, and different preparation methods can lead to different surface amounts of titania on the silica matrix, hydroxyl groups or surface defects [11–14].

Scope of the study

The aim of this study was to investigate the behaviour of aromatic molecules close to the titania–silica surface. The molecules chosen for investigation differ in their functional groups—they contain different numbers of electrostatically charged atoms (–CH_3, –OH, –COOH). Such analysis can provide useful information about the types of intermolecular interactions that are of importance in adsorption occurring on different adsorption centres.

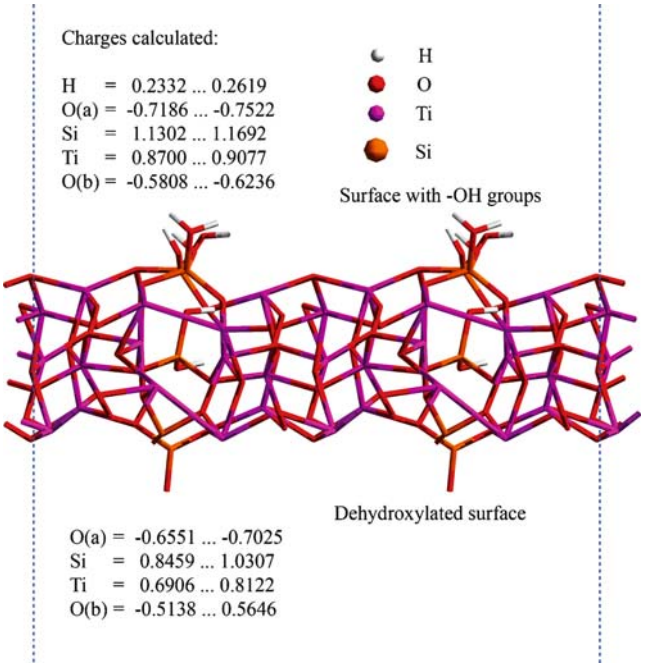

Fig. 1 Model used in simulations, and charges assigned to selected atoms. *O(a)* Oxygen atom from –O–Si–O– bridge, *O(b)* oxygen atom from Ti–O surface

Model and computational details

Construction of the model of the catalyst used in the study was based on cell parameters and atom coordinates of anatase taken from the Cerius^2 model library [15].

The size of the model was increased to that of four elementary cells of anatase, with those units being connected via –O–Si–O– groups so as to create two atomic surfaces. On the one side of this structure, hydrogen atoms were added to form hydroxyl groups, while the other surface remained dehydroxylated (Fig. 1). This model was subsequently optimised to ensure its minimal energy.

Charges calculated for all atoms in the system indicate that the hydroxylated surface is more electrostatically active. For example, charges on oxygen atoms in –O–Si–O– bridges vary from −0.7186 to −0.7522 on the hydroxylated surface, thus are more negative than on the other surface of the catalyst, where they vary from −0.6551 to −0.7025. Similarly, the charges on Ti and Si atoms are more positive on the hydroxylated surface than on the relevant atoms on the surface without hydroxyl groups.

The model consisted of approximately 1,000 atoms. For such models the only choice for determining the potential energy is the forcefield method, which yields reliable results at a comparatively low computational cost.

The forcefield data give an expression describing the potential energy surface for a given model as a function of atomic coordinates. The total potential energy of the system (E_{total}) is expressed as the sum of the energy resulting from the chemical bond length (E_{bond}), the energies of angle bending (E_{angle}) and dihedral angle bending (E_{dihedral}) between atoms, and the energy of the cross-terms describing the interactions between lengths and angles ($E_{\text{cross-term}}$). If the system consists of more than one molecule, a term describing the energy of nonbonding van der Waals (E_{vdW}) and Coulomb (E_{Coulomb}) interactions is introduced. Then we have:

$$E_{\text{total}} = E_{\text{bond}} + E_{\text{angle}} + E_{\text{dihedral}} + E_{\text{cross-term}} + E_{\text{vdW}} + E_{\text{coulomb}}$$

Hence we have the terms describing the non-bonding interactions that are the most important in adsorption: van der Waals and electrostatic. In Universal forcefield (UFF) [16–18], which we have chosen for simulations (as in the work of Toulhoat et al. [19]), van der Waals interactions are described with Lennard–Jones 6–12 type expression.

Recent work by Sagara et al. [20] as well as Yang and Zhong [21] point to the fact that UFF simulations lead to unusually high loading of guest molecules in the sorbate micropores. Since we aim to study the differences in behaviour of chosen molecules in proximity to the catalyst surface rather than loading itself, we assume that this does not influence our results.

To analyse the adsorption phenomenon, we made use of the Grand Canonical Monte Carlo (GCMC) ensemble [22, 23]. In the course of the simulation process, the chemical potential (μ), the volume of the system (V) and temperature (T) were kept constant. The method involves multiple

sampling of the guest molecule position in the micropores of the host. The state obtained in this way is accepted with a probability depending on the energy of a system in this state. The procedure is repeated a sufficient number of times such that is statistically significant and enables the thermodynamical equilibrium to be achieved.

In order to simulate the phenomenon of adsorption of aromatic compounds on a surface of a TiO_2/SiO_2 catalyst, we chose phenol, toluene, salicylic acid and benzoic acid as the model adsorbates. Considering the ease with which these molecules produce a variety of conformers, we established a library comprising ten such conformers prior to the main simulation procedure.

The GCMC simulations were repeated at pressures varying from 0.125 kPa to 8 kPa and temperatures ranging between 273 K and 323 K. The number of steps, which was chosen according to the pressure applied, varied from one million to two million.

Results and discussion

Isotherms of the adsorption of the investigated guest molecules are presented in Fig. 2. They suggest that the adsorption behaviour of toluene and phenol molecules is similar. In the case of toluene, adsorption is rapid when a certain pressure value is exceeded. Both 298 and 323 K isotherms indicate that almost all adsorption sites are occupied at pressures above 2 kPa, while only a few molecules are present in the system at pressures below 0.5 kPa. Very similar behaviour can be observed with phenol present in the system. The adsorption isotherm curve also indicates fast adsorption after exceeding a certain pressure value; however, the number of adsorbed molecules increases gradually, i.e. the slope of the adsorption isotherm is not as steep as in the case of toluene. Increasing the volume of the electrostatically charged parts of the molecule (–OH, –COOH, and both these groups in phenol, benzoic acid and salicylic acid) causes adsorption to occur progressively. Moreover, adsorption of salicylic acid starts at lower pressure values than that of benzoic acid or phenol within the investigated range. Hence we may conclude that electrostatic host–guest interactions facilitate the adsorption of benzene derivatives, especially at low pressure.

Analysis of mass cloud visualisations confirmed the strong interactions between adsorbate molecules. In all cases guest molecules tended to concentrate in groups; however, the host-guest interaction energy differs for different molecules. Figure 3 presents the different characters of adsorbate interactions with the host surface. Toluene

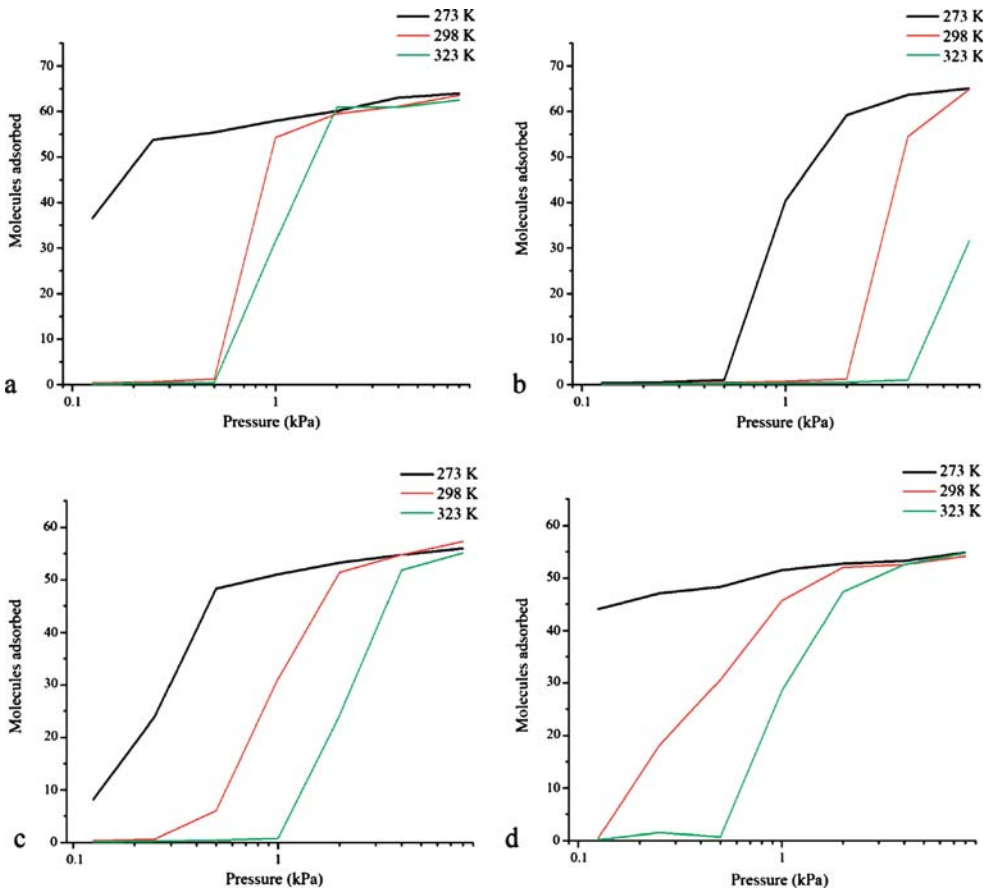

Fig. 2a–d Adsorption isotherms of aromatic compounds. **a** Toluene, **b** phenol, **c** benzoic acid, **d** salicylic acid

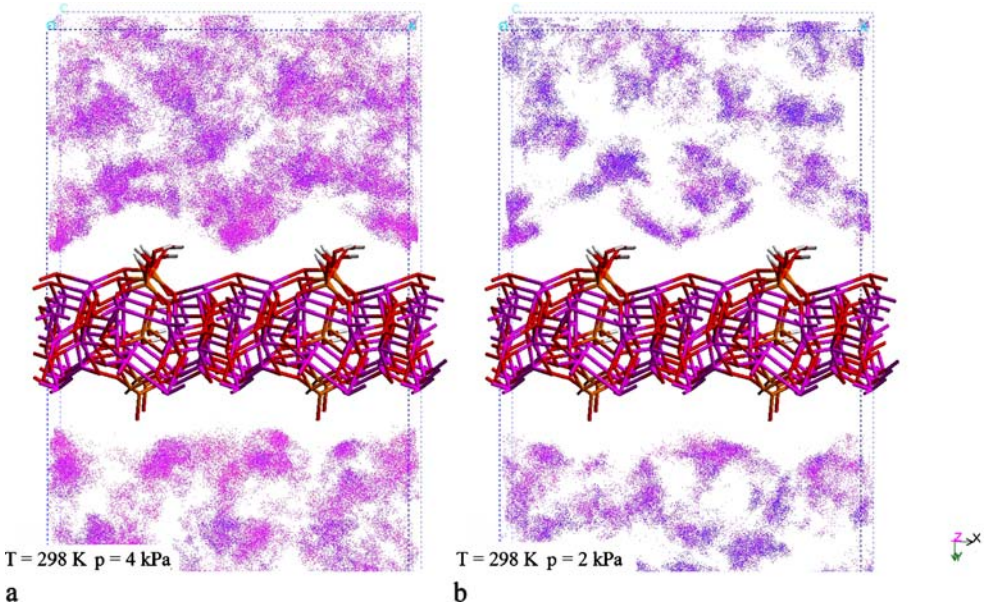

Fig. 3 Mass cloud visualisations of **a** phenol and **b** toluene

can be adsorbed on both hydroxylated and dehydroxylated surfaces of the TiO_2/SiO_2 catalyst and molecules of toluene occupying adsorption centres have lower host–guest interaction energy than in the case of phenol molecules. Similarly, when phenol is introduced into the system, its molecules start to occupy the entire space above the catalyst surface. Moreover host–guest interaction energies are higher than in the case of toluene. The presence of more "concentrated" mass clouds of toluene (Fig. 3) allow the conclusion that adsorbed molecules change their position only slightly while within the range of interaction of the adsorption centre. In this case, the behaviour of phenol is different—the molecules are not immobilised at the adsorption centres. Moreover, if we take into account the higher interaction energy at sites near the surface than at sites located further away, we can conclude that interactions

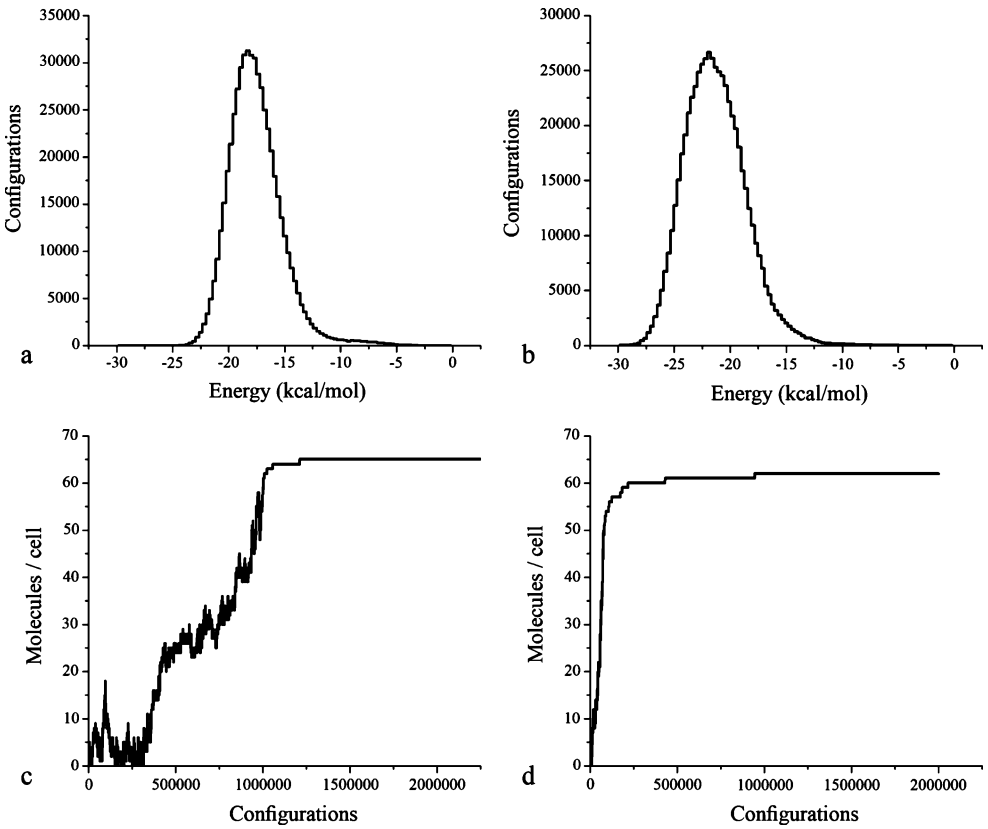

Fig. 4 Energy distribution histograms and loading curves of phenol (**a**, **c**) and toluene (**b**, **d**)

between phenol molecules are of greater importance than host–guest interactions.

Intermolecular interactions between organic molecules also seem to play an important role in toluene adsorption, as evidenced by the loading curves shown in Fig. 4. Although the number of phenol molecules is slightly larger when compared to the number of toluene molecules, the character of the interaction of guest molecules with the TiO_2/SiO_2 surface is very similar. Molecules of phenol strongly attract each other and it seems also in this case that those interactions prevail over host–guest interactions. However, host–guest interaction energy is higher in the case of phenol than in the case of toluene, which results in slower (more iterations needed) attainment of the equilibrium state and stronger immobilisation of toluene molecules at the adsorption centres.

The adsorption of benzoic acid molecules is more complex. The energy distribution indicates that the initial steps of the simulation process lead to the adsorption of molecules at centres with relatively high host–guest interaction energy—which may seem strange, because low-energy sites should be occupied first. Further simulation shows that adsorbate locations of lower energy than in the initial part of simulation are occupied. This behaviour can be explained by enabling low-energy adsorption sites by preadsorption. Initially, after introducing adsorbate to the system, only few aromatic molecules are present, and these are in close contact with the TiO_2/SiO_2 surface (as shown in Fig. 5). The energy distribution shows that during the first 600,000 steps of simulation (blue line) host–guest interaction energy is relatively high. The location of these molecules is shown in the Fig. 5b as red dots close to the catalyst surface. These preadsorbed molecules enable the sites with low energy to be accessed by other molecules. Analysis of benzoic acid adsorption at 298 K and 500 Pa revealed the presence of three maxima at about −8, −15 and −20 kcal mol^{-1}. Mass cloud analysis confirmed that only in the case of the −8 kcal mol^{-1} maximum (corresponding to the initial stage of adsorption) do molecules adsorb at both surfaces of the catalyst—the next stages of adsorption occur only on/above the hydroxylated surface. However, it was not possible to localise surface centres corresponding

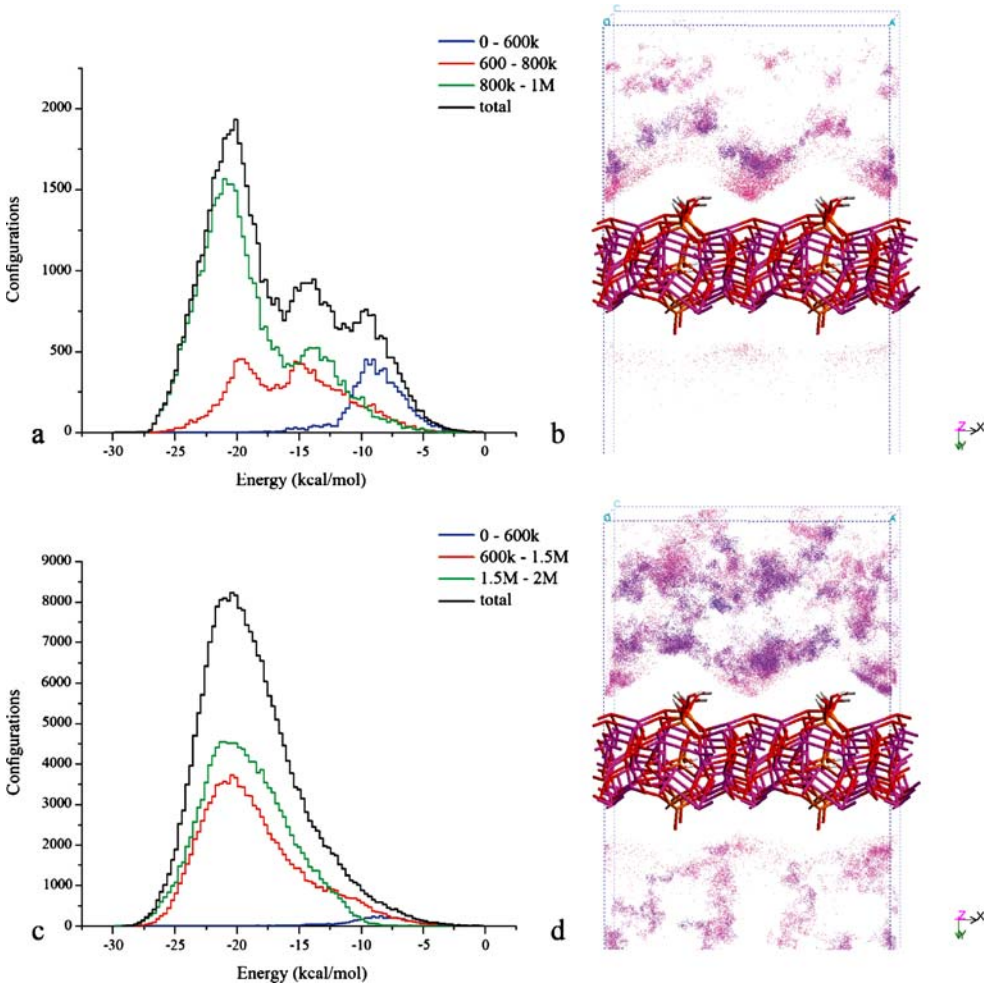

Fig. 5a–d Energy distribution histograms and mass cloud visualisations of benzoic acid. **a**, **b** Temperature (T) = 298 K, pressure = 500 Pa; **c**, **d** T=323 K, pressure 2 kPa

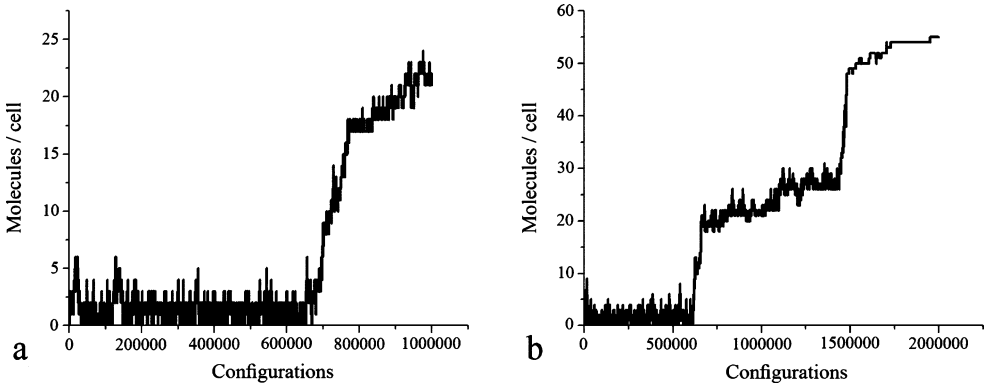

Fig. 6 **a**, **b** Loading curves of benzoic acid. **a** T=298 K, pressure = 500 Pa; **b** T=323 K, pressure = 2 kPa

precisely to the −15 and −20 kcal mol^{-1} maxima, due to the simultaneous occurrence of adsorption on both of these sites.

The loading curve of benzoic acid (Fig. 6b) supports the observation that at the very beginning of the simulation there are only a few molecules of adsorbate close to the surface centres of the catalyst. When these molecules adsorb to the active centre they form the first layer; this is followed by adsorption of species at a greater distance from the catalyst surface.

The behaviour of salicylic acid is similar to that of benzoic acid; however, electrostatic interactions are even more important. As shown in Fig. 7, molecules of salicylic acid adsorb to the hydroxylated surface much more easily. At a temperature of 323 K and pressure 0.25 kPa (Fig. 7a), only the hydroxylated surface is occupied by organic molecules. Under these conditions loading is very low (approximately 1 molecule per supercell), and mass cloud represents the best adsorption sites available. Similarly, under 0.5 kPa pressure and a temperature of 298 K (Fig. 7b), most molecules of salicylic acid are located on the hydroxylated surface of catalyst. If we raise the pressure to 1 kPa at the same temperature, molecules start to occupy the other side of catalyst, which has no hydroxyl groups. But even then the preference of the hydroxylated surface is apparent—more blue dots over the hydroxylated surface indicate that the energy of adsorption is lower than in the case of the surface without hydroxyl groups.

Conclusions

Interactions between adsorbing molecules played an important role in all investigated species. Increasing the volume of electrostatically non-inert functional groups of a molecule led to better adsorption; electrostatic host–guest interactions prevail over van der Waals interactions. The hydroxylated surface is preferred during adsorption; however, it seems that in the case of phenol the presence of hydroxyl groups on the TiO_2/SiO_2 surface does not influence adsorption. Adsorption isotherms supported by loading curves revealed multilayer adsorption in the case of larger molecules (benzoic acid and salicylic acid). Rapid adsorption occurs in the case of phenol and toluene after exceeding the limiting pressure value, while adsorption of benzoic and salicylic acids increases slowly with very small

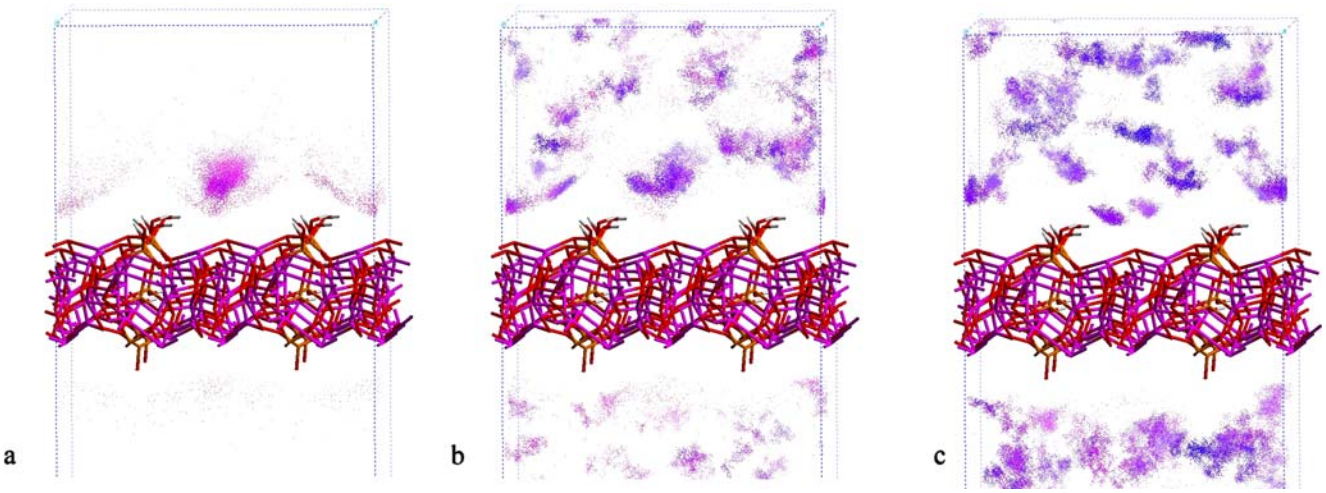

Fig. 7 **a**–**c** Mass cloud visualisations of salicylic acid at various temperatures and pressures. **a** 323 K and 0.25 kPa; **b** 298 K and 0.5 kPa; **c** 298 K and 1 kPa

changes in pressure. Toluene and phenol occupy all possible sites from the very beginning of the simulation, especially under high pressure; there is no difference between adsorption sites (close/far from the surface, or the presence or absence of hydroxyl groups).

Acknowledgments This work is supported by the Polish Ministry of Education and Science (Grant no.3 T09B 03 228).

All calculations were carried out in the Wrocław Centre of Networking and Supercomputing in Wrocław, Interdisciplinary Centre for Mathematical and Computational Modeling in Warsaw and Academic Computer Centre "Cyfronet" in Cracow.

References

1. Fujishima A, Honda K (1972) Nature 238:37–38
2. Kaneko M, Okura I (2002) Photocatalysis: science and technology, Springer/Kodansha, Tokyo
3. Linsebigler AL, Lu G, Yates JT (1995) Chem Rev 95:735–758
4. Moon SC, Matsumura Y, Kitano M, Matsuoka M, Anpo M (2003) Res Chem Intermed 29:233–256
5. Peral J, Domenech X, Ollis DF (1997) Chem Technol Biotechnol 70:117–140
6. Fujishima A, Rao TN, Tryk DA (2000) J Photochem Photobiol C 1:1–21
7. Bhatkhande DS, Pangarkar VG, Beenackers AACM (2001) J Chem Technol Biotechnol 77:102–116
8. Bacsa RR, Kiwi J (1998) Appl Cat B 16:19–29
9. Zhang Q, Gao L, Guo J (2000) Appl Cat B 26:207–215
10. Xu Y, Zheng W, Liu W (1999) J Photochem Photobiol A 122:57–60
11. Yoda S, Otake K, Takebayashi Y, Sugeta T, Sato T (2001) J Non-Cryst Solids 285:8–12
12. Davis RJ, Liu Z (1997) Chem Mater 9:2311–2324
13. Malinowska B, Walendziewski J, Robert D, Weber JV, Stolarski M (2003) Appl Catal B 46:441–451
14. Brodzik K, Walendziewski J, Stolarski M, Van Ginneken L, Elst K, Meynen V (2006) J Porous Mater (in press). Published online 29 December 2006, DOI 10.1007/s10934-006-9027-9
15. Cerius^2—Materials Science Tutorial Guide (1995) BIOSYM/Molecular Simulations
16. Casewit CJ, Colwell KS, Rappe AK (1992) J Am Chem Soc 114:10035–10046
17. Casewit CJ, Colwell KS, Rappe AK (1992) J Am Chem Soc 114:10046–10053
18. Rappe AK, Colwell KS, Casewit CJ (1993) Inorg Chem 32:3438–3450
19. Toulhoat H, Raybaud P, Benazzi E (2004) J Catal 221:500–509
20. Sagara T, Klassen J, Ganz E (2004) J Chem Phys 121:12543–12547
21. Yang Q, Zhong C (2005) J Phys Chem B 109:11862–11864
22. Woods GB, Panagiotopoulos AZ, Rowlinson JS (1988) Mol Phys 63:49–63
23. Razmus DM, Hall CK (1991) AIChE J 37:769–775